Journal of Power Sources 202 (2012) 11–17

Contents lists available at SciVerse ScienceDirect

Journal of Power Sources

journal homepage: www.elsevier.com/locate/jpowsour

Comparison of electrochemical stability of transition metal carbides (WC, W_2C, Mo_2C) over a wide pH range

Mark C. Weidman, Daniel V. Esposito, Yeh-Chun Hsu, Jingguang G. Chen*

Center for Catalytic Science and Technology, Department of Chemical Engineering, University of Delaware, Newark, DE 19716, United States

ARTICLE INFO

Article history:
Received 15 September 2011
Received in revised form 23 October 2011
Accepted 24 October 2011
Available online 15 November 2011

Keywords:
Tungsten carbides (WC, W_2C)
Molybdenum carbide (Mo_2C)
Electrochemical stability
E-pH diagram
Cyclic voltammetry (CV)
Chronopotentiometry (CP)

ABSTRACT

Transition metal carbides have shown potential for use in electrochemical applications as low-cost catalysts or catalyst support materials. In order to determine which transition metal carbides are suitable for specific electrochemical applications, it is necessary to determine their stability in electrolytic solutions of varying pH values. In this work we compare the stability of the most commonly used carbides: tungsten carbides (WC and W_2C) and molybdenum carbide (Mo_2C). Cyclic voltammetry (CV) is used to determine the onset of oxidation and the hydrogen evolution reaction (HER) at discrete pH values while chronopotentiometric (CP) titrations are used to create potential-pH 'stability maps', which designate the regions of stability, passivation, and oxidation. Based on the slopes of the boundaries between the regions of stability, information about the oxidation mechanisms is obtained through the Nernst equation, indicating key differences in the electrochemical behavior of each surface. WC exhibits enhanced resistance to surface oxidation in acidic solution and comparable stability in neutral/alkaline solution to Mo_2C and W_2C.

1. Introduction

Transition metal carbides have been studied for potential use as electrocatalysts and electrocatalyst supports in a variety of electrochemical devices including fuel cells, electrolyzers, photoelectrochemical cells, and capacitors [1–8]. In addition to being more abundant and less expensive than the Pt-group metal catalysts [9], transition metal carbides have demonstrated favorable activity and stability for many applications [10]. The carbides of group VI transition metals such as tungsten (W) and molybdenum (Mo) are of particular interest as electrocatalysts. It is important to note, however, that the electrochemical properties of carbides can vary greatly depending on operating conditions (electrochemical potential, current density) as well as pH environment (acidic, neutral, basic). Therefore, it is of particular interest to understand the electrochemical stability of transition metal carbide catalysts over a wide range of conditions to determine their utility for various electrochemical applications.

Pourbaix diagrams present the thermodynamically stable state of a material at different potential and pH values. Such information is necessary for understanding the stability of transition metal carbides; however, Pourbaix diagrams are typically only available for pure elements. Nevertheless, the Pourbaix diagrams for metallic W and Mo can still provide useful information, as some or all of the behavior of parent metals likely extends to their carbide forms. Both W and Mo have Pourbaix diagrams that exhibit similar E-pH regions of stability and corrosion [11–13]. In general, there are three distinct regions of stability identified in the W and Mo Pourbaix diagrams. At potentials more negative than the reversible hydrogen potential, the surfaces of W and Mo are most stable in their metallic state, and are reported to be immune from corrosion. At more positive potentials, the oxidation of the surfaces starts to occur, with the nature of the oxidation process depending on the pH of the solution. In an acidic environment, W is converted to WO_3 at sufficiently positive potentials. Likewise, Mo is oxidized to MoO_3 in the pH region between 0 and 1. A small degree of surface oxidation can sometimes be beneficial for a catalyst. For example, it has been reported that a slightly oxidized WC surface displays higher catalytic activity towards the electrooxidation of certain fuels or hydrogen adsorption on the surface [14–16]. When the surface becomes slightly oxidized, it is considered to be passivated. As operating potentials increase further, the material enters the sustained oxidation region, where corrosion occurs. Sustained oxidation is typically detrimental to the performance of the electrocatalyst and should be avoided [17]. At neutral and alkaline conditions, neither W- or Mo-oxide species are stable and form ions that dissolve into solution. When operating in neutral or basic solution, W and Mo oxides formed on the surfaces of the electrode are continuously dissolved, resulting in a loss of catalyst material. This region is therefore referred to as the surface oxidation/dissolution

* Corresponding author. Tel.: +1 302 831 0642; fax: +1 302 831 2085.
E-mail address: jgchen@udel.edu (J.G. Chen).

0378-7753/$ – see front matter © 2011 Elsevier B.V. All rights reserved.
doi:10.1016/j.jpowsour.2011.10.093

region. An important difference between W and Mo is that Mo exhibits a state of active corrosion in acidic environments while W does not. In the pH region of approximately 0–3, Mo can form Mo^{3+} in a certain potential range. While the information available from Pourbaix diagrams pertains to W and Mo, it is anticipated that some of this behavior should extend to the carbides of W and Mo.

With increasing interests and efforts in utilizing tungsten and molybdenum carbides as alternative electrocatalysts [5–7], it is critical to understand the stability threshold of these carbides under different ranges of pH and potential values. In the current study we provide a detailed comparison of the E-pH regions of stability for WC, W_2C and Mo_2C under wide ranges of pH and potential values. The primary objective of the current work is to identify stable regions for the electrocatalytic applications of tungsten and molybdenum carbides. This work is a follow up to a previous study in which the stability regions of tungsten monocarbide (WC) were determined as well as the potentials where WC begins to catalyze the hydrogen evolution reaction (HER) [18]. Transition metal carbides have shown promise as inexpensive catalysts for performing this reaction [16,19]. In the current paper we extend these studies to W_2C and molybdenum carbide (Mo_2C). Standard electrochemical analysis techniques are used to determine when each catalyst material begins to catalyze the HER as well as to undergo surface oxidation. The technique of chronopotentiometric (CP) titration is used to determine the stability of these catalysts over a wide pH range. Compared to conventional Pourbaix diagrams, the CP titration technique offers several potential advantages. First, a Pourbaix diagram is based on thermodynamically stable states and thus neglects the kinetics of the reactions occurring. They are also not typically available for multi-component materials such as the transition metal carbides studied here. By using the CP titration technique, a pseudo-Pourbaix diagram can be created for a wider range of materials with specific solution conditions. This technique can be used to quickly create an E-pH diagram or 'stability map' for a given material and electrolyte conditions, identifying stable regions for which that material may be suitable for a specific electrochemical application.

2. Experimental

2.1. Electrode synthesis

All electrodes were synthesized from their parent metal substrates, W and Mo foils (both Alfa Aesar, 99.95%). WC and Mo_2C were synthesized directly through carburization in a Lindberg furnace (model 55035). The details of the WC synthesis have previously been published [18]. The production of Mo_2C begins with Mo being heated to 250 °C over the course of 2 h and then to 850 °C over 4 h. The temperature was then held constant at 850 °C for 1 h. This process was performed in the presence of methane and hydrogen gas at flow rates of 66 and 122 sccm, respectively. After 1 h of sustained heating at 850 °C the methane feed was shut off to prevent formation of excess surface carbon and the samples were allowed to cool to room temperature in a hydrogen environment. This synthesis process serves to drive carbon into the bulk of the Mo and the parameters were based on those found in literature [20]. W_2C was synthesized through physical vapor deposition (PVD) by magnetron sputtering of a WC target onto W foil substrates. The samples were then annealed to 825 °C in the Lindberg furnace with flow rates of 33 and 122 sccm methane and hydrogen, respectively. After being heated at 825 °C for 1 h the methane feed was shut off and the sample was held at this temperature for an additional 30 min. This was followed by a cooling period in which only the hydrogen flow rate was maintained. All carbide samples were passivated at room temperature for 2 h in a 1% O_2/99% N_2 gas mixture before being exposed to atmospheric conditions.

The bulk crystal phases of the carbide thin films were determined using symmetric X-ray diffraction (XRD) and glancing incidence XRD (GIXRD). XRD was performed using a Phillips X'Pert PW3040-MPD X-ray diffractometer operated with a Cu Kα X-ray source at 45 kV and 40 mA. GIXRD was obtained using a Rigaku D/Max 2200 diffractometer with a Cu Kα source operated at 40 mA and 40 kV. Measurements were conducted with an incident angle of 5°, which corresponds to a sampling depth of approximately 350 nm for WC/W_2C samples.

2.2. Electrochemical measurements

A Princeton Applied Research VersaSTAT V4 was used as the potentiostat/galvanostat for electrode testing. A standard three-neck setup was employed with Pt mesh (Alfa Aesar, 99.9%) serving as the auxiliary electrode. The reference electrode was a saturated potassium chloride calomel electrode (SCE, +0.241 V vs. normal hydrogen electrode). All potentials are reported with respect to the SCE. The electrolyte used consisted of 0.1 M phosphoric acid buffer (H_3PO_4, Sigma–Aldrich, ≥85%) and 0.1 M sodium sulfate (Na_2SO_4, Fischer Scientific, 99.3%) in deionized water purified to resistance below 17 MΩ cm by a Barnstead NANOpure filtration system. Sulfuric acid (H_2SO_4, Fischer Scientific, 96.9%) and sodium hydroxide (NaOH, Fischer Scientific, 99.5%) were chosen for changing the pH values of the electrolyte solution. Although Na^+ and SO_4^- are relatively benign counter ions, 0.1 M Na_2SO_4 was added to each solution to ensure the presence of both ions, regardless of solution pH. The pH value of a solution was determined using an Accumet Portable Laboratory AP61 pH meter.

Electrochemical solutions were purged with nitrogen gas for approximately 30 min to remove oxygen from solution prior to testing. Nitrogen was continuously swept over the surface of the three-neck cell during experiments. Before use, all electrodes were treated with 0.3 M NaOH solution followed by rinsing with acetone, methanol, and DI water. This treatment was previously shown to be effective at removing surface oxides accumulated on the electrode surface prior to the experiment [18].

3. Results and discussion

3.1. Electrode characterization

Fig. 1 presents GIXRD and symmetric XRD patterns of W_2C and Mo_2C samples. The GIXRD measurements probe to a depth of approximately 350 nm, while the symmetric XRD measurements characterize much deeper into the bulk of the material. Reflecting this difference in sampling depth, diffraction peaks originating from the metal substrates (W, Mo) are clearly visible in the symmetric XRD measurements but are absent in GIXRD spectra, indicating that the carbide layers are at least 350 nm in thickness. The phase purity of the carbide films has been verified with patterns from the International Center for Diffraction Data (ICDD) for W_2C [ICDD 00-035-0776] and Mo_2C [ICDD 00-035-0787]. The GIXRD patterns for the three samples confirm that each thin film is comprised of a single carbide phase.

3.2. Mapping E-pH regions of stability for WC, W_2C, and Mo_2C

Chronopotentiometric (CP) titrations were performed with WC, W_2C, and Mo_2C electrodes from an initial pH value of 0.5 up to a final value of about 12 in order to create E-pH stability diagrams for these materials. A detailed procedure for the CP titration technique has been previously published elsewhere [18]. Briefly, the CP measurements consist of holding the current density of the working electrode constant at 0.0 or 0.1 mA cm^{-2} while recording the electrochemical potential versus the reference electrode. After a

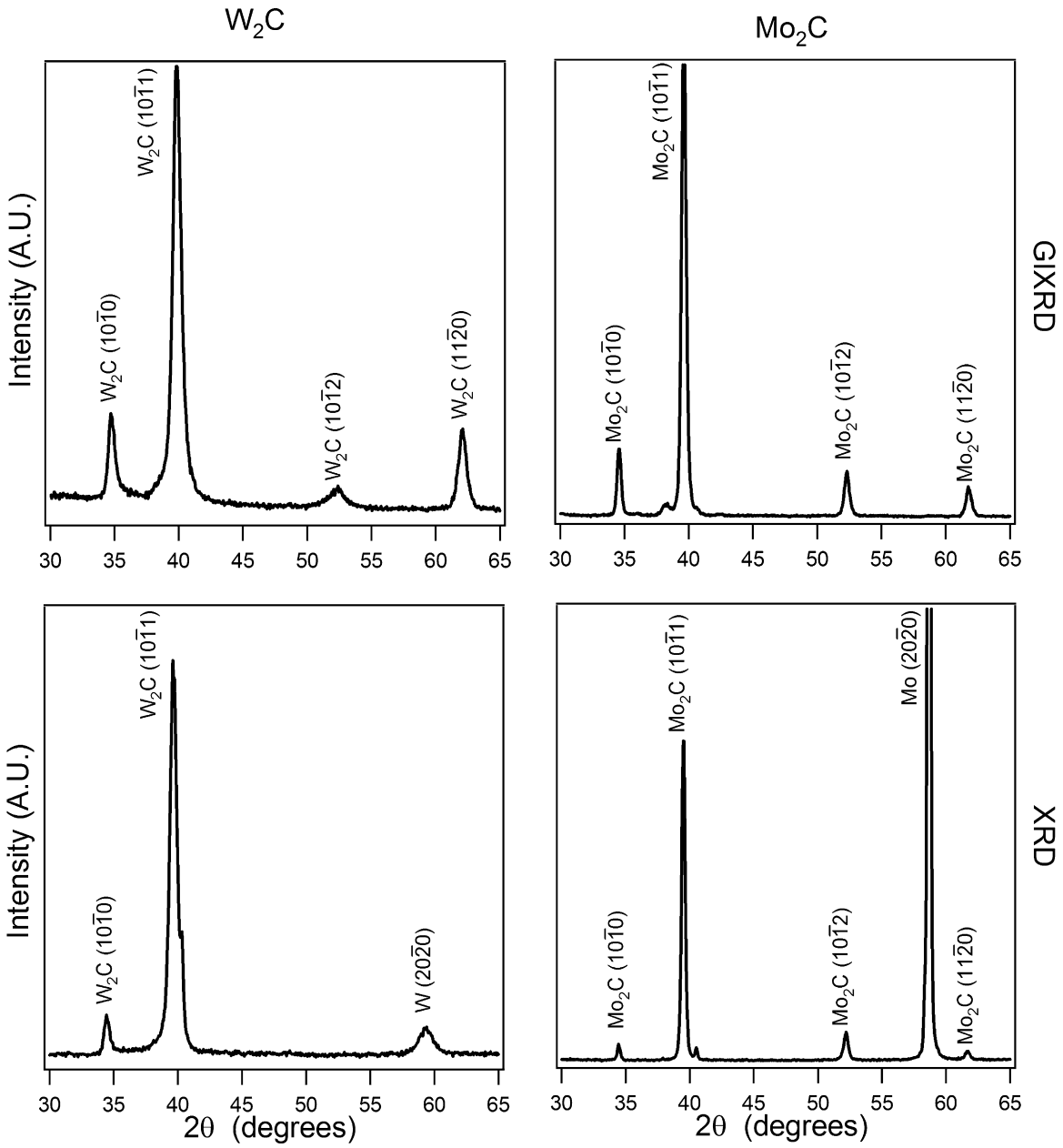

Fig. 1. GIXRD (top row) and XRD (bottom row) of W_2C and Mo_2C. GIXRD penetration depth is approximately 350 nm while XRD characterizes much deeper into the bulk material.

steady state potential is reached at the initial pH of 0.5, the solution pH is incrementally increased through the addition of a small aliquot of concentrated base titrant. Following each titration step, the solution pH and electrode potential are again allowed to equilibrate, at which point both data points are recorded. The diagrams thus generated are useful for determining different regions of stability, similar to a Pourbaix diagram. The technique is similar to chronoamperometric (CA) titration measurements previously used in the literature for evaluation of corrosion behavior [12,18].

CP titrations are shown for W_2C and Mo_2C thin film electrodes in Fig. 2, with titration curves conducted at current densities of 0.0 mA cm^{-2} and 0.1 mA cm^{-2}; for comparison, similar CP curves of WC from a previous study [18] are also included in Fig. 2. At 0.0 mA cm^{-2} the oxidation and reduction reactions on the electrode surface are equal, creating a baseline curve of the open circuit potential as a function of pH. At potential values more negative than the 0.0 mA cm^{-2} titration curve, the electrode surface can be considered to be relatively immune to oxide formation, and at exceedingly negative potentials, the HER is catalyzed for the three carbides. The second titration curve was carried out with a constant current density of 0.1 mA cm^{-2}. Potentials more positive than the 0.1 mA cm^{-2} curve should result in significant surface oxidation or dissolution, depending on the solution pH. This region should typically be avoided as it leads to degradation of the catalyst. The region that is bounded by the 0.0 mA cm^{-2} and 0.1 mA cm^{-2} curves can be considered to approximate the passivation region on the E-pH diagram. It is within the passivation region that the material could function without much risk to surface oxidation or dissolution. As discussed in the introduction, Mo is known to form Mo^{3+} under similar conditions and it is a possibility that Mo_2C exhibits the same behavior [11]. This possibility is further investigated in Section 3.3.

The three carbides in Fig. 2 show similar trends in their E-pH stability based on the CP titrations, with large regions of passivation at low pH values and narrow passivation regions in neutral

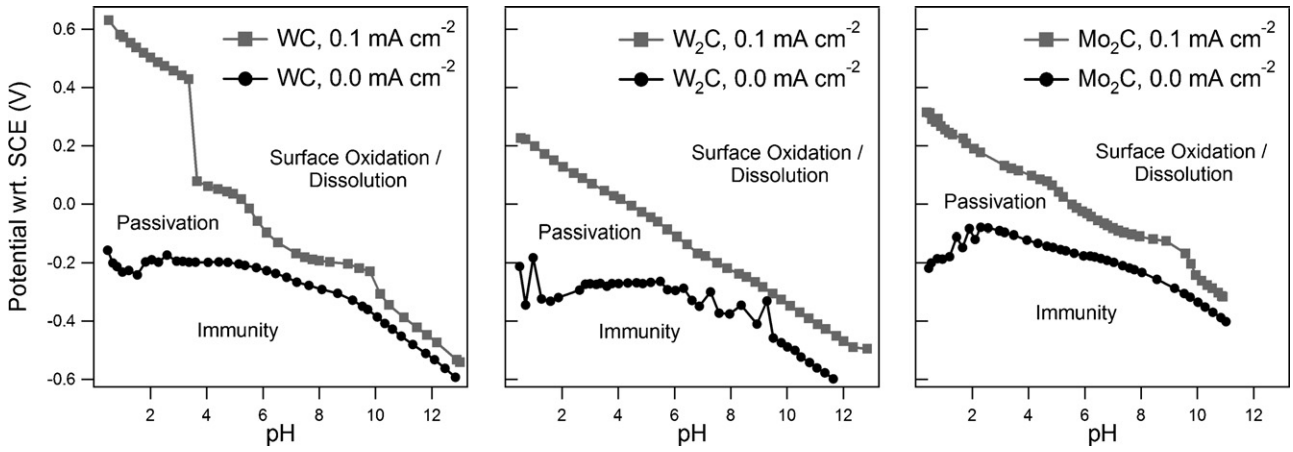

Fig. 2. Comparison of CP titration experiments for stability mapping on WC, W_2C, and Mo_2C. Samples were held at 0.0 mA cm^{-2} and 0.1 mA cm^{-2} to outline the regions of immunity, passivation, and surface oxidation/dissolution. The titration curves of WC [18] are included for comparison.

and alkaline solutions. Although all three carbides have similar oxidation onset potentials and passivation regions at neutral and alkaline pH values, WC exhibits a notably larger region of stability in the pH range of 0.5-4.0. In acidic environments, WC has a large span of potentials at which it could operate without undergoing severe surface oxidation. WC could therefore be useful for a variety of applications whose operating conditions fall within this region. In comparison, W_2C and Mo_2C show smaller regions of passivation in acidic environments. All three carbides have similar behavior as solution conditions become neutral or alkaline; at these pH values the surface oxides are unstable and the passivation region diminishes.

Also of interest in Fig. 2 are the slopes of the CP titration curves, which contain information about the reaction mechanism by which an electrode material is oxidized. The theoretical link between reaction mechanism and the slope of an E-pH curve is the Nernst equation, which relates the reversible reaction potential, E, to the stoichiometric coefficients (ν) and activities (a) of the reductant and oxidant species that partake in a given reaction:

$$E = E^{o} - \frac{RT}{nF} \ln\left(\frac{\Pi a_{\text{red.}}^{\nu}}{\Pi a_{\text{oxid.}}^{\nu}}\right) \quad (1)$$

In Eq. (1), R is the universal gas constant, T is the temperature, F is the Faraday constant, E^o is the standard reduction potential of the reaction of concern, and n is the stoichiometric number of electrons involved in the reaction. For an oxidation reaction in which H^+ is an oxidant species (or OH^- is a reductant species), the theoretical rate of change of electrode potential with respect to pH, $d(E)/d(\text{pH})$, can be obtained by taking the derivative of Eq. (1). At 298 K, this expression is given by:

$$\frac{d(E)}{d(\text{pH})} = -\left(\frac{\nu_{H^+}}{n}\right) \times (59.1 \quad \text{mV} \quad \text{pH unit}^{-1}) \quad (2)$$

where the slope is observed to be dependent on the ratio of stoichiometric coefficients for H^+ and the number of e^-. Although the CP titrations in Fig. 2 were not carried out under thermodynamic equilibrium, the low current densities and steady state nature of the CP titration experiment justify a comparison of the measured $d(E)/d(\text{pH})$ to the theoretically expected values obtained from Eq. (2).

To compare the measured $d(E)/d(\text{pH})$ to that expected from Eq. (2), a linear fit was made to all of the 0.1 mA cm^{-2} titration curves in Fig. 2, in addition to that for metallic W, which was recently published [18]. The calculated slopes are listed for each electrode in Table 1. For the W and W_2C electrodes, the 0.1 mA cm^{-2} CP curves were very linear across the entire pH range, for which a single slope was calculated. Both slopes are close to the theoretical value of −59.1 mV pH unit^{-1} (corresponding to $(\nu_{H^+}/n) = 1$). The good agreement of $d(E)/d(\text{pH})$ across the entire pH range indicates that these two electrode materials undergo a corrosion mechanism or mechanisms at this current density for which (ν_{H^+}/n) of the kinetically limited step(s) remains constant with a value of ~1.0. In contrast to W and W_2C, the 0.1 mA cm^{-2} CP curves for WC and Mo_2C electrodes exhibit multiple linear regions with varying slopes, suggesting that several different reaction mechanisms are kinetically important across the pH range. For both WC and Mo_2C, five pH regions with distinct linear slopes were observed, with the slopes for each region included in Table 1.

In Table 2, commonly considered corrosion mechanisms are provided for WC, W_2C, and Mo_2C electrodes, along with the corresponding (ν_{H^+}/n) and $d(E)/d(\text{pH})$ values based on Eq. (2). The reactions listed in Table 2 are not meant to represent a comprehensive set of possible corrosion mechanisms for these materials, but have been identified as important reactions based on literature [14,21–23] and/or their likely occurrence based on thermodynamically stable products from the W and Mo Pourbaix diagrams [11]. In the latter case, CO_2 and CO_3^{2-} were assumed to be the stable product for the carbidic carbon in acidic and alkaline solutions, respectively. A comparison of the calculated slopes in Table 1 with the expected values of $d(E)/d(\text{pH})$ in Table 2 leads to several good matches. Although the calculated CP slopes cannot be used by themselves to conclusively identify specific reaction mechanisms, it is possible to

Table 1
Calculated slopes for 0.1 mA cm^{-2} CP titration curves over defined pH ranges for W, W_2C, WC, and Mo_2C electrodes. Slopes were obtained from linear regression over the defined pH range.

Sample	pH range	Slope (mV pH unit^{-1})
W	1.3–13.0	−58.0
W_2C	0.3–13.0	−59.7
WC	0.5–3.4	−62.5
	3.7–5.2	−36.4
	5.5–6.5	−112.5
	7.2–9.8	−20.5
	10.2–13.0	−80.2
Mo_2C	0.4–2.3	−71.3
	3.2–4.8	−38.6
	5.1–7.2	−60.6
	7.4–8.9	−18.6
	9.6–10.9	−102.1

Table 2
List of possible reactions involved with the corrosion of W, W_2C, WC, and Mo_2C electrodes, along with the corresponding (ν_{H^+}/n) and $d(E)/d(pH)$ according to Eq. (2). The reaction types are classified by (ν_{H^+}/n) and are described in the text.

Reaction		Electrode	Overall reaction	(ν_{H^+}/n)	$d(E)/d(pH)$ [mV pH unit^{-1}]
No.	Type				
1	i	W	$W + 3H_2O \rightarrow WO_{3(s)} + 6H^+ + 6e^-$	1.00	−59.1
2	i		$W + 2H_2O \rightarrow WO_{2(s)} + 4H^+ + 4e^-$	1.00	−59.1
3	ii		$W + 4H_2O \rightarrow WO^{2-}_{4(aq)} + 8H^+ + 6e^-$	1.33	−78.8
4	i	WC	$WC + 5H_2O \rightarrow WO_3 + CO_2 + 10H^+ + 10e^-$	1.00	−59.1
5	i		$WC + 4H_2O \rightarrow WO_{2(s)} + CO_2 + 8H^+ + 8e^-$	1.00	−59.1
6	ii		$WC + 14OH^- \rightarrow WO^{2-}_4 + CO^{2-}_3 + 7H_2O + 10e^-$	1.40	−82.7
7	i	W_2C	$W_2C + 8H_2O \rightarrow 2WO_3 + CO_2 + 16H^+ + 16e^-$	1.00	−59.1
8	i		$WC + 4H_2O \rightarrow WO_{2(s)} + CO_2 + 8H^+ + 8e^-$	1.00	−59.1
9	ii		$W_2C + 22OH^- \rightarrow 2WO^{2-}_4 + CO^{2-}_3 + 11H_2O + 16e^-$	1.38	−81.3
10	iii	W, WC, or W_2C	$WO_{3(s)} + OH^- \rightarrow WO^{2-}_{4(aq)} + H^+$	∞	−∞
11	i		$WO_{2(s)} + H_2O \rightarrow WO_{3(s)} + 2H^+ + 2e^-$	1.00	−59.1
12	ii		$WO_{2(s)} + 2H_2O \rightarrow WO^{2-}_{4(aq)} + 4H^+ + 2e^-$	2.00	−118.2
13	i	Mo_2C	$Mo_2C + 8H_2O \rightarrow 2MoO_{3(s)} + CO_2 + 16H^+ + 16e^-$	1.00	−59.1
14	iv		$Mo_2C \rightarrow 2Mo^{3+} + CO_2 + 6e^-$	0.00	0.0
15	i		$Mo_2C + 6H_2O \rightarrow MoO_{2(s)} + CO_2 + 12H^+ + 12e^-$	1.00	−59.1
16	ii		$Mo_2C + 10H_2O \rightarrow 2MoO^{2-}_{4(aq)} + CO_2 + 20H^+ + 16e^-$	1.25	−73.9
17	iii		$MoO_{3(s)} + OH^- \rightarrow MoO^{2-}_{4(aq)} + H^+$	∞	−∞
18	ii		$MoO_{2(s)} + 2H_2O \rightarrow MoO^{2-}_{4(aq)} + 4H^+ + 2e^-$	2.00	−118.2

identify the type of reaction taking place based on measured $d(E)/d(pH)$. The requirement to maintain a charge balance in a given chemical equation ensures that certain types of reactions will always have characteristic $d(E)/d(pH)$ slopes. Four such types of reactions and their relation to $d(E)/d(pH)$ are listed below:

i. H^+ or OH^- mediated oxidation reactions that result in the transformation of metal into a charge-neutral, solid oxide-product are characterized by $(\nu_{H^+}/n) = 1$ and a corresponding slope of $d(E)/d(pH) = -59.1$ mV pH unit^{-1}.
ii. Oxidation reactions that produce dissolved metal-oxide anions and are characterized by $(\nu_{H^+}/n) > 1.0$ and $d(E)/d(pH) < -59.1$ mV pH unit^{-1}.
iii. Chemical reactions, for which no electrons are transferred between the electrode and the solution. When mediated by H^+ or OH^-, these reactions are characterized by $(\nu_{H^+}/n) = \infty$ and $d(E)/d(pH) = \infty$ mV pH unit^{-1}.
iv. Oxidation reactions that are not mediated by H^+ or OH^- are characterized by $(\nu_{H^+}/n) = 0$ and $d(E)/d(pH) = 0$ mV pH unit^{-1}.

Based on the slopes of the 0.1 mA cm^{-2} CP titration curves in Table 1 and the characteristic slopes of the four reaction types listed above, the following broad conclusions can be made concerning the oxidation of the W, W_2C, WC, and Mo_2C electrodes:

(1) The corrosion of W and W_2C electrodes is kinetically limited by the formation of solid W-oxide surface species throughout the entire pH range (0.5–13.0), as evidenced by the constant slope of $d(E)/d(pH) \sim -59$ mV pH unit^{-1} for the 0.1 mA cm^{-2} CP curves.
(2) The step-change in potential for the 0.1 mA cm^{-2} CP curve of WC at pH ∼ 3 is consistent with chemical reaction (10) in Table 2, dissolution of WO_3 to tungstate ions, becoming dominant.
(3) Oxidation reactions of the WC and Mo_2C electrodes appear to be kinetically limited by the dissolution or further oxidation of the surface oxide species, as evidenced by the measured $d(E)/d(pH)$ regions that are far less or far greater than −59.1 mV pH unit^{-1}. This may indicate that the W and Mo oxides formed on these electrodes are more strongly adhered to the underlying WC and Mo_2C layers than those formed on the W and W_2C electrodes. This suggestion is corroborated by the substantially larger passivation region observed for the WC electrode at low pH in Fig. 2, but raises the question of why a similar increase in the passivation region is not observed for Mo_2C at low pH values.

It is important to keep in mind that the above analysis of the kinetically limited reaction steps based on the slopes of 0.1 mA cm^{-2} CP titration curves is only applicable to the specific conditions used for these experiments. Other experimental conditions, such as temperature, hydrodynamic control, and CP current density are likely to have a strong influence on the kinetically limiting step. For example, increased flow rates of the electrolyte over the electrode surface are likely to aid in the removal of surface oxides, possibly making the oxide formation mechanism rate-limiting in certain situations.

3.3. CV characteristics at select pH values

CV measurements were performed on W_2C and Mo_2C thin film electrodes at solution pH values of 0.5, 2.5, 6.0, 9.0, 11.0, and 13.0. The 25th cycle of CV is presented for all samples. Scans were performed at a rate of 50 mV s^{-1}. At all pH values the Mo_2C thin film does not exhibit an oxidation onset potential until ∼0.1 V more positive than W_2C (slightly less at pH of 0.5), consistent with the CP titrations of Fig. 2. In the CV curves of the Mo_2C electrode at pH of 0.5 and 2.5, no anodic current is observed at these intermediate potentials, which should be present if the active corrosion mechanism to Mo^{3+}, as reported for the Mo metal, was occurring in the current study. Therefore there is no evidence of active corrosion on the Mo_2C electrode from the experiments performed in this work. Nevertheless, further investigation into this possible corrosion mechanism is warranted for Mo_2C catalysts, especially in long term stability studies for which very low corrosion rates may become more apparent.

From the CV measurements of Fig. 3 it was possible to extract the approximate onset potentials towards surface oxidation (+0.1 mA cm^{-2}) and the HER (−0.1 mA cm^{-2}) at the six pH values studied. These potentials were also determined from CV cycles on WC, not presented here [18]. The onset potential values for WC, W_2C, and Mo_2C are given in Fig. 4 along with the reversible potentials of the HER and oxygen evolution reaction (OER) as determined by the Nernst equation. In Fig. 4, all three carbides are seen to catalyze the HER with similar overpotentials (∼150 mV) over the entire pH range. These overpotential losses are significantly larger

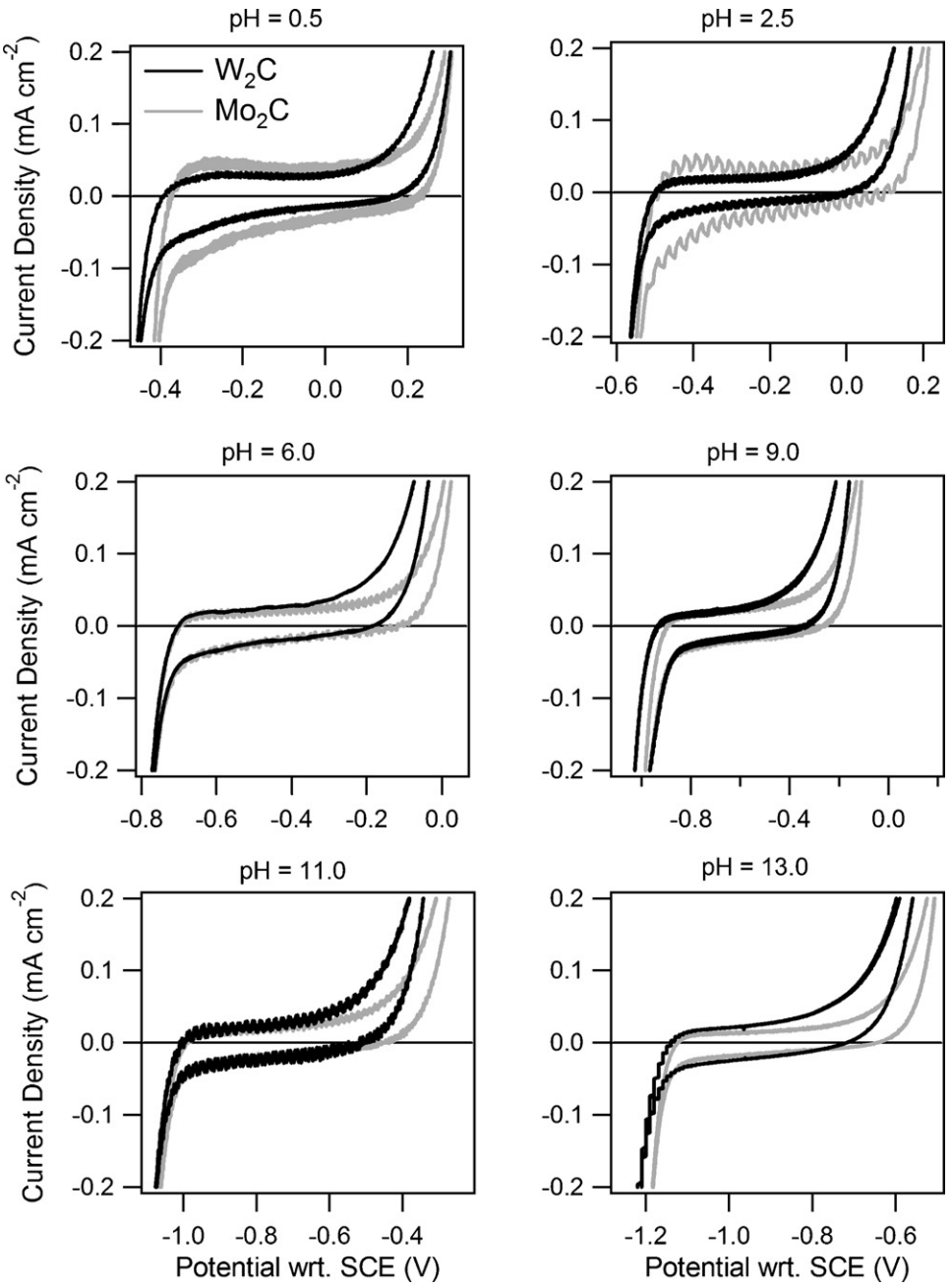

Fig. 3. CV on W_2C (black) and Mo_2C (gray) at pH values of 0.5, 2.5, 6.0, 9.0, 11.0, and 13.0. 25th cycles shown, scan rate of 50 mV s^{-1}.

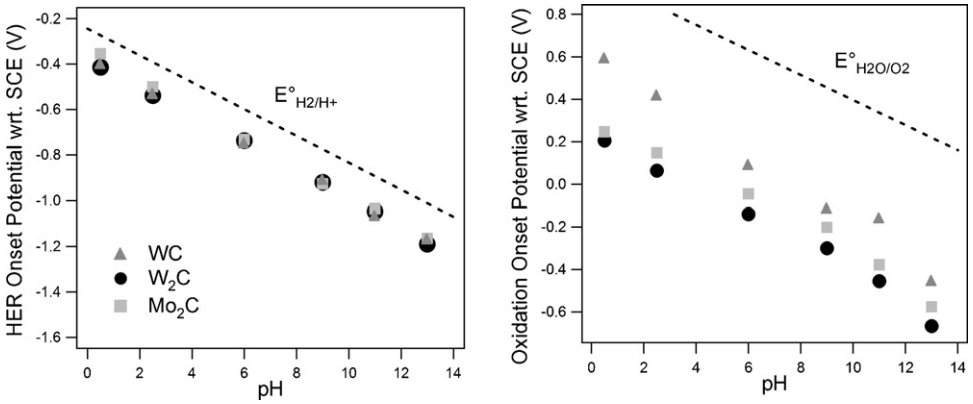

Fig. 4. HER onset and oxidation onset potentials for WC (triangles), W_2C (circles), and Mo_2C (squares) over the pH range. Values were based on when CV cycles first reached -0.1 mA cm^{-2} and +0.1 mA cm^{-2} for HER and surface oxidation, respectively.

than those incurred by commonly employed precious metal HER catalysts, but still small enough to warrant consideration of these carbide materials as stand-alone HER catalysts [19,24,25]. This is especially true for low current density applications, such as photoelectrochemical cells, for which overpotential losses will remain limited. In other applications for which the HER activity of carbides is insufficient, carbides may be used as stable supports for monolayer amounts of precious metal HER catalysts, thereby reducing precious metal loading while maintaining high HER activity [7]. Results from the current study also indicate that W_2C and Mo_2C should be stable under the typical E-pH values used for HER, which in turn suggest the possibility of utilizing W_2C and Mo_2C as catalyst supports.

When considering the onset of oxidation in Fig. 4, the three carbides are predicted to undergo oxidation before oxygen evolution begins. Furthermore, WC shows excellent resistance to oxidation at pH values of 0.5 and 2.5 as compared to W_2C and Mo_2C. In neutral and alkaline solutions, the trend in stability is $WC > Mo_2C > W_2C$, although the difference appears to be relatively small. The CP titration measurements in Fig. 2 do not show a significant difference between the $0.1\,mA\,cm^{-2}$ curves in these pH regions, suggesting that the slight differences in oxidation onset potentials as determined by the CV do not translate to a noticeably larger passivation operating region.

4. Conclusions

The carbides of Group VI transition metals show similar stability behavior over wide ranges of solution pH. WC exhibits the largest region of stability at low pH, as determined by the CP titration and CV measurements, making it an attractive material as catalyst and catalyst support in acidic environments. WC, W_2C, and Mo_2C have comparable regions of passivation in neutral/alkaline solutions. From the $0.1\,mA\,cm^{-2}$ CP titration curves, the calculated slopes were compared to theoretical values of $d(E)/d(pH)$ for commonly considered corrosion reactions of each material. This analysis suggested that corrosion of W_2C is kinetically limited by the formation of surface oxide species under the tested conditions over the whole pH range, while the CP curves for the WC and Mo_2C electrodes showed various slopes indicating that different types of reactions are kinetically limiting in different pH regimes. In terms of hydrogen evolution activity, the carbide catalysts studied here have comparable overpotentials and could be used for this application. The data presented in this study should be useful for identifying the pH and potential limits for the electrochemical application of these carbide catalysts.

Acknowledgements

We acknowledge financial support from the Department of Energy (DE-FG02-00ER15104). We also acknowledge partial support from the Office of Naval Research (ONR Grant # 00014-08-1-0423). MCW acknowledges financial support from the Barry M. Goldwater Scholarship and Excellence in Education Program.

References

[1] D.J. Ham, J.S. Lee, Energies (2009) 873–899.
[2] H.H. Hwu, J.G. Chen, Chem. Rev. 105 (2005) 185–212.
[3] S.T. Oyama, The Chemistry of Transition Metal Carbides and Nitrides, Blackie Academic and Professional, Glasgow, 1996.
[4] E.C. Weigert, J. South, S.A. Rykov, J.G. Chen, Catal. Today 99 (2005) 285–290.
[5] A. Serov, C. Kwak, Appl. Catal. B: Environ. 90 (2009) 313–320.
[6] E. Antolini, E.R. Gonzalez, Appl. Catal. B: Environ. 96 (2010) 245–266.
[7] D.V. Esposito, J.G. Chen, Energy Environ. Sci. 4 (2011) 3900–3912.
[8] E.C. Weigert, A.L. Stottlemyer, M.B. Zellner, J.G. Chen, J. Phys. Chem. C 111 (2007) 14617–14620.
[9] C.J. Yang, Energy Policy 37 (2009) 1805–1808.
[10] R.B. Levy, M. Boudart, Science 181 (1973) 547–549.
[11] M. Pourbaix, Atlas of Electrochemical Equilibria in Aqueous Solutions, National Association of Corrosion Engineers, Houston, TX, 1974.
[12] M. Anik, K. Osseo-Asare, J. Electrochem. Soc. 149 (2002) B224–B233.
[13] M.P. Zach, K. Inazu, K.H. Ng, J.C. Hemminger, R.M. Penner, Chem. Mater. 14 (2002) 3206–3216.
[14] J.D. Voorhies, J. Electrochem. Soc. 119 (1972) 219.
[15] Y.Y. Shao, J. Liu, Y. Wang, Y.H. Lin, J. Mater. Chem. 19 (2009) 46–59.
[16] D.V. Esposito, S.T. Hunt, A.L. Stottlemyer, K.D. Dobson, B.E. McCandless, R.W. Birkmire, J.G. Chen, Angew. Chem. Int. Ed. 49 (2010) 9859–9862.
[17] F. Harnisch, U. Schroder, M. Quaas, F. Scholz, Appl. Catal. B: Environ. 87 (2009) 63–69.
[18] M.C. Weidman, D.V. Esposito, I.J. Hsu, J.G. Chen, J. Electrochem. Soc. 157 (2010) F179–F188.
[19] F. Harnisch, G. Sievers, U. Schroder, Appl. Catal. B: Environ. 89 (2009) 455–458.
[20] D.C. LaMont, A.J. Gilligan, A.R.S. Darujati, A.S. Chellappa, W.J. Thomson, Appl. Catal. A: Gen. 255 (2003) 239–253.
[21] B. Bozzini, G.P. De Gaudenzi, A. Fanigliulo, C. Mele, Corros. Sci. 46 (2004) 453–469.
[22] A. Maslennikov, C. Cannes, B. Fourest, N. Boudanova, V. Vivier, P. Moisy, Radiochim. Acta 95 (2007) 339–408.
[23] M. Anik, Corros. Sci. 48 (2006) 4158–4173.
[24] D.V. Sokolsky, V.S. Palanker, E.N. Baybatyrov, Electrochim. Acta 20 (1975) 71–77.
[25] I. Nikolov, K. Petrov, T. Vitanov, A. Guschev, Int. J. Hydrogen Energy 8 (1983) 437–440.